

Voltametric Investigation of the CT-DNA Interaction with Bioactive Metal Chelates. Part. I. Chelated Nickel(II) Isatin-Hydrazone Complexes

Mostafa K. Rabia*, Nabawia M. Ismail, Ahmad Desoky M. Mohamad and Ali Abdo Mahmoud

Chemistry Department, Faculty of Science, Sohag University, 82534 Sohag, Egypt.

Received: 5 Nov. 2015, Revised: 6 Dec 2015, Accepted: 7 Dec. 2015.

Published online: 1 Jan. 2016.

Abstract: The new synthesized bioactive Ni(II) isatin-hydrazone complexes have been investigated in presence of Britton–Robinson buffer “universal buffer” as supporting electrolyte, using at glassy carbon electrode. The CV of these complexes is characterized by one cathodic peak in the forward direction at -0.535 V and one anodic peak in the reverse direction at 0.811 V. The two waves considered as two independently irreversible cyclic voltammetric peaks. The CT-DNA binding property of the Ni(II) isatin-hydrazone complexes has also been characterized using cyclic voltammetry under physiological conditions (pH 7.4 and 25 ± 0.2 °C). As a result of the interaction of the subject complexes with CT-DNA, a considerable decrease in the peak currents and a significant shift in the peak potentials were observed. These changes in the cyclic voltammetric characteristics of Ni(II) isatin-hydrazone complexes indicated that these complexes bind to CT-DNA by intercalative mode with intrinsic binding constants in the range of 10^{-4} M⁻¹.

Keywords: Ni(II) isatin-hydrazone complexes, cyclic voltammetry, CT-DNA binding.

1 Introduction

Transition metal ions are playing an important role in biological processes in the human body [1,2]. For example, nickel (II) ions are one of the most abundant transition metals in humans. They are found either at the active sites or as structural components of a good number of enzymes [3,4].

In the other hand, a variety of biological activities including analgesic [5], anticonvulsant [6], antidepressant [7], anti-inflammatory [8], antimicrobial, and effects on the central nervous system [9] are associated with isatin hydrazones and Pyridine derivatives. Isatins are capable of crossing the blood–brain-barrier [10], influence neurodegenerative diseases, participate in metabolism, acetylcholine esterase inhibitors and stimulate the growth of plants [11]. Drugs containing the isatin skeleton are used to treat diseases such as epilepsy [12], tuberculosis [13], and bulimia [14]. Pyridine derivatives play significant role in many biological systems as the component of several vitamins, nucleic acids, enzymes and proteins [15].

The study of the coordination chemistry of biologically important metal ions with hydrazone ligands has been one of the recent developments in the field of bioinorganic

chemistry. Therefore the need to create novel isatin derivatives for emerging drug targets is an active area of medicinal chemistry. Studies on the interaction of these complexes and DNA are rare in literature. Thus, our interest is in the synthesis and structural characterization of new bioactive isatin-hydrazone complexes. We previously synthesized and characterized new isatin-hydrazone compounds derived from isatin monohydrazone and 2-pyridyl, which show notable biological activity [16]. In addition we have also been synthesized and reported in detail their Ni(II) complexes [17], with evaluation of their anti-bacterial and anti-fungal activity [18]. The interaction of these complexes with CT-DNA by spectroscopic and viscometric measurements has also been investigated in our laboratory [18]. In the current interest, this paper has reported the cyclic voltammetric characterization of the Ni(II) isatin-hydrazone complexes and their interaction with CT-DNA. The electrochemical parameters and binding constants were calculated and discussed

2. Experimental

2.1. Chemicals.

Universal buffer (Britton–Robinson buffer) was used as supporting electrolyte in the cyclic voltammetric characterization of the Ni(II) complexes. It was prepared

* Corresponding author E-mail: mostafarabia@hotmail.com

with various pH values from 100 cm³ of mixed acid solution, containing 0.04 mol L⁻¹ of each of boric acid, ortho-phosphoric acid and acetic acid in de-ionized water, sodium hydroxide solution (0.5 mol.L⁻¹) was used to adjust pH values. Calf thymus (CT-DNA) and Tris[hydroxymethyl]aminomethane (2-amino-2-hydroxymethyl-propane-1,3-diol) (Tris) were purchased from Sigma-Aldrich Chemie. The CT-DNA was dissolved in Tris-HCl buffer pH 7.4. For preparation of the Tris-HCl buffer pH 7.4, Trizma base (1.2114 g) was dissolved in 80 ml de-ionized water, adjust the pH to 7.4 with the appropriate volume of concentrated HCl then bring the final volume to 100 cm³ with de-ionized water and finally autoclave and store at room temperature. Other chemicals were of analytical reagent grade.

2.2. Synthesis of the Isatin-hydrazone Ligands and Their Ni(II) Complexes

The Isatin-hydrazone ligands, namely [(pyridine-2-carboxaldehyde)-3-isatin]-bishydrazone (cpish), [(2-acetyl pyridine)-3-isatin]-bishydrazone (apish), and [(2-benzoyl pyridine)-3-isatin]-bishydrazone (bpish), and their Ni(II) complexes were prepared as described in our previous work [16,17,18]. The schematic diagram of the prepared Ni(II) isatin-hydrazone complexes with are shown in scheme (1).

2.3. Cyclic voltammetric measurements

2.3.1. Apparatus

Cyclic voltammograms of the complexes were recorded under nitrogen gas using a Potentiostat/Galvanostat (model 173). The cell contains three electrodes; Glassy-carbon electrode, (0.245 cm²), was employed as a working electrode, Saturated Calomel Electrode (SCE) was used as reference electrode and platinum wire was used as counter electrode.

2.3.2. Measurement of the active surface area of the working electrode

The active surface area of the Glassy-carbon working electrode was determined by performing the cyclic voltammetric of the Glassy-carbon working electrode in 20 mM [Fe(CN)₆]³⁺ and 0.2 M KCl at 0.020 V.s⁻¹ versus saturated calomel electrode as reference electrode. The well-defined reduction and oxidation peaks due to the Fe³⁺/Fe²⁺ redox couple were noticeable versus saturated calomel electrode as reference electrode in forward and reverse scans, respectively. The electro active surface was determined according to Randles-Sevcik equation [19].

$$I_p = 2.69 \times 10^5 AD^{1/2} n^{3/2} \nu^{1/2} C$$

Where n is the number of electrons participating in the redox reaction ($n=1$), A is the area of the electrode (cm²), D is the diffusion coefficient of the probe molecule in solution (6.70 x10⁻⁶ cm² s⁻¹) [20], C is the concentration of the probe

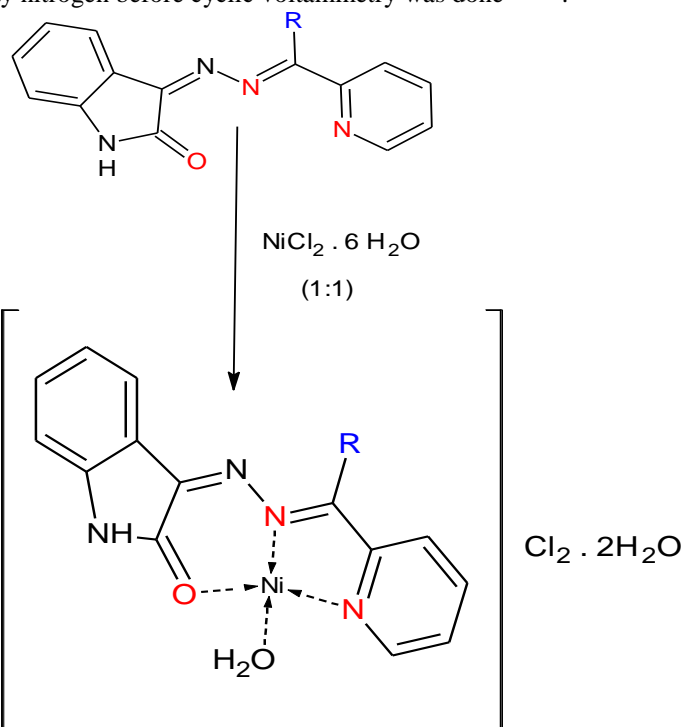
in bulk solution (mol cm⁻³), and ν is the scan rate (V s⁻¹).

2.3.3. Cyclic voltammetric Procedure

In order to provide a reproducible active surface and to improve the sensitivity and resolution of the voltammetric peaks, the glassy carbon electrode was polished on a smooth polishing cloth and then rinsed with methanol and double distilled water prior to each electrochemical measurements. Before each measurement the solutions were de-aerated by a stream of pure nitrogen gas for 16 min. During the measurements, nitrogen was passed above the solutions in the cell. All experiments were carried out at ambient temperature (25 ± 1 °C).

2.3.4. DNA-binding using Cyclic Voltammetry.

Cyclic voltammetric experiments were done in absence and presence of 10, 20, 30, 40, 50 μM of CT-DNA in 10% aqueous methanol solution in universal buffer (pH 7.4), using Potentiostat/Galvanostat (Model 173). All experimental solutions were degassed for 30 min with high-purity nitrogen before cyclic voltammetry was done [21,22].



Scheme (1): Schematic diagram of the Ni(II)Isatin-hydrazone complexes, R=H, cpish; R=CH₃, apish ; R=ph, bpish.

3. Results and discussion

3.1. Cyclic Voltammetric studies of the prepared Ni(II) complexes

The electrochemical behavior of the newly synthesized Ni(II) complexes have been investigated in 10% aqueous-methanol (v/v), Britton–Robinson buffer “universal buffer” as supporting electrolyte. Glassy carbon electrode, GCE, saturated Calomel electrode, SCE, and platinum wire are used as working, reference and counter electrodes, respectively.

The cyclic voltammograms, CV, are performed in a potential window of 1.5 to -1.4 volt, at wide range of scan rates from 0.080 to 1.0 V/s and at different values of pH, from 2.8 to 8.2. Furthermore a wide range of the Ni(II) complex concentrations, from 2 to 12 μM are used. The cyclic voltammetric data are assembled in Table (1). Analysis of these data is presented as follows;

3.1.1. Effect of Scan Rate

Fig. (1); Shows the cyclic voltammogram, CV, of the $[\text{Ni}(\text{cpish})(\text{H}_2\text{O})]\text{Cl}_2 \cdot 2\text{H}_2\text{O}$ complex, as representative example, in a potential range of 1.5 to -1.4 volt, at range of scan rates from 0.080 to 1.0 V/s and pH 7.4. The subject complex shows one irreversible cathodic wave at -0.535 V, the oxidation counterpart is lacking and one irreversible anodic wave at 0.811 V versus S.C.E. The peak to peak separation, ΔE_p , of these two waves is in the range of 1000 to 1300 mV, which increases with increasing of the scan rate. These values of ΔE_p , show that the two C.V waves are independently irreversible in nature.

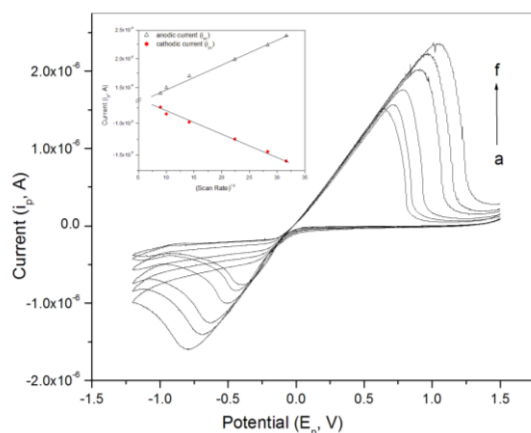


Fig. (1), Cyclic voltammogram of 7.0 μM $[\text{Ni}(\text{cpish})(\text{H}_2\text{O})]\text{Cl}_2 \cdot 2\text{H}_2\text{O}$ complex in 10% aqueous methanol (v/v) in universal buffer at pH 7.4 at different scan rates; a. 0.080, b. 0.100, c. 0.200, d. 0.500, e. 0.800 and f. 1.000 V/s, and the inserted figure shows the relation of the peak current with the square route of the scan rate for both cathodic, i_{pc} , and anodic, i_{pa} , peak currents.

As shown from the inserted figure in fig. (1), the peak current relations of both cathodic and anodic waves with scan rates are constructed. It is found that, the peak currents, i_{pc} and i_{pa} , are directly proportional to the square root of scan rate, $v^{1/2}$, with correlation coefficients of 0.99 and 0.98 respectively. This indicates that, the cathodic and anodic processes of the subject complex are diffusion controlled in nature [23]. The diffusion coefficient, D, of the Ni(II) isatin-hydrazone complexes is estimated from the slop of the following equation [24].

$$i_p = (2.99 \times 10^5) n(\alpha n)^{1/2} AC(Dv)^{1/2}$$

Where, α , is the transfer coefficient, n is the number of transferred electrons, A is the area of the glassy carbon electrode (cm^2), v is the scan rate (mV/s) and C is the concentration of the solution (mol/cm^3). α_n is calculated from the following equation [25];

$$\alpha n = \frac{-47.7}{E_p - E_{p/2}}$$

The diffusion coefficient of the subject complexes calculated for n=1, are cited in table (1).

A linear least squares fit of $\log i_p$ verses $\log v$ for both cathodic and anodic waves, c. f. fig. (2), are obtained with slope of 0.46 and 0.45 and correlation coefficients, r, of 0.998 and 0.98, respectively. Each of these linear least squares can be represented by the following;

$$\log i_p = -5.69 + 0.46 \log v \quad (\text{reduction})$$

$$\log i_p = -5.23 + 0.45 \log v \quad (\text{oxidation})$$

These indicate that the two CV waves are diffusion controlled processes.

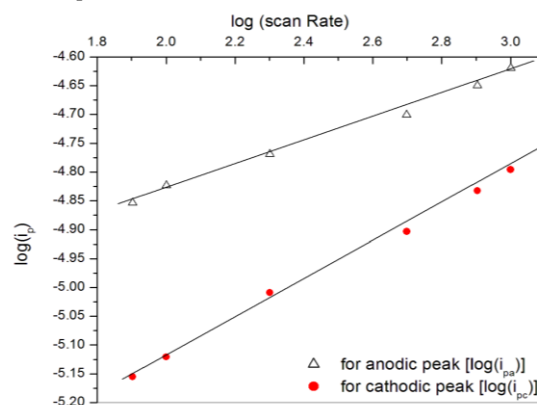


Fig. (2), Relation of log (peak current), i_{pc} and i_{pa} , of $[\text{Ni}(\text{cpish})(\text{H}_2\text{O})]\text{Cl}_2 \cdot 2\text{H}_2\text{O}$ complex with $\log(v)$.

Furthermore, the peak potential, E_p , of the cathodic wave, E_{pc} , shifts to more negative potential, while the anodic one, E_{pa} , shifts to more positive potentials on increasing the scan rate, c. f. fig. (3). The best estimated least squares equations obtained for the two CV waves are formulated by the following equations;

$$E_{pc} (\text{V}) = 0.094 - 0.293 \log v \quad (\text{reduction wave})$$

$$E_{pa} (\text{V}) = 0.231 + 0.257 \log v \quad (\text{oxidation wave})$$

The slop values are 0.293 and 0.257 for the cathodic

and anodic CV waves respectively. These data suggest that, the two CV waves are due to ir-reversible one-electron transfer processes followed by a chemical reaction.

Moreover, the dependence of the current function, $i_p/v^{1/2}$, on the scan rate, v , is an important dramatic to establishing the type of mechanism. To achieving this objective, the CVs of the complexes were recorded at various scan rates. The corresponding data of the complexes are listed in Table (1). The effect of scan rate on complex, $[\text{Ni}(\text{cpish})(\text{H}_2\text{O})]\text{Cl}_2 \cdot 2\text{H}_2\text{O}$, is shown in fig. (1). The shift in peak potential with the increase in scan rate manifests the irreversibility of the reduction and oxidation processes.

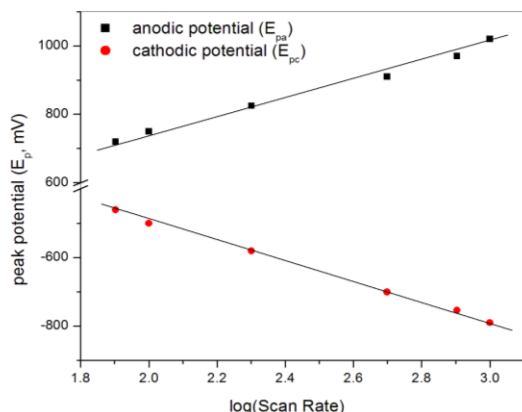


Fig. (3), Relation of (peak potential), E_{pc} and E_{pa} , of $[\text{Ni}(\text{cpish})(\text{H}_2\text{O})]\text{Cl}_2 \cdot 2\text{H}_2\text{O}$ complex with $\log(v)$.

3.1.2. Effect of pH

The pH of the supporting electrolyte has a significant effect on the redox behavior of the complexes. Fig. (4), represents the effect of pH on the cyclic voltammetric behavior of the $[\text{Ni}(\text{cpish})(\text{H}_2\text{O})]\text{Cl}_2 \cdot 2\text{H}_2\text{O}$ complex, as a representative example, in universal buffer, at pH range from 2.8 to 8.2. It is shown that, by changing the pH of the solution, a variation of the cyclic voltammetric response of the subject complexes is observed. Both of the reduction and the oxidation peaks are observed in the whole pH range of the study for pH range from 2.8 to 8.2. The voltammetric peak current, i_p , and peak potential, E_p , for both cathodic and anodic peaks of the $[\text{Ni}(\text{cpish})(\text{H}_2\text{O})]\text{Cl}_2 \cdot 2\text{H}_2\text{O}$ complex depend on the pH of the solution. From fig. (5), it is observed that, at lower pHs (< 3) and at higher pHs (> 8) the $[\text{Ni}(\text{cpish})(\text{H}_2\text{O})]\text{Cl}_2 \cdot 2\text{H}_2\text{O}$ complex is decomposed. On the other hand, the subject complex has high stability at neutral pH value, $\text{pH} = 7.24$, c.f. fig. (5). On plotting of the peak potential, E_p , vs. pH (2.8-8.2) shows one a straight line. This can be expressed by the following equations, c.f. the inserted figure in fig. (4),

$$E_p (\text{V}) = -0.535 - 0.012 \text{ pH}, \quad r = 0.977 \quad (\text{Reduction peak})$$

$$E_p (\text{V}) = 0.756 + 0.014 \text{ pH}, \quad r = 0.998 \quad (\text{Anodic peak})$$

The effect of pH on peak current of all the complexes at pH 2.8 – 8.2 has also been evaluated. On increasing the pH of the solution, the peak current, i_{pa} and i_{pc} , increases until the peak current, i_p , reaches a maximum value at $\text{pH} = 7.4$, then the peak current, i_p , decreased, c.f.

fig. (5). This change in the peak current is associated with a shift in the cathodic peak potential, E_{pc} , to more negative direction and a shift in the anodic peak potential, E_{pa} , to more positive direction, c.f. the inserted figure in fig. (4). The best and sharpest peak and reproducible results have been obtained at pH 7.4. Therefore, this medium has been chosen in this study as the supporting electrolyte for the electrochemical investigation.

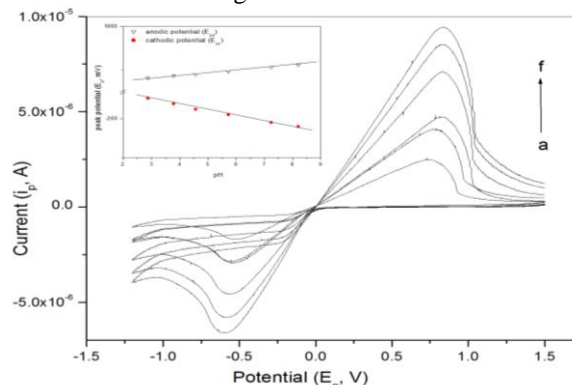


Fig. (4), Cyclic voltammogram of $7.0 \mu\text{M}$ $[\text{Ni}(\text{cpish})(\text{H}_2\text{O})]\text{Cl}_2 \cdot 2\text{H}_2\text{O}$ complex in 10% aqueous methanol (v/v) in universal buffer at scan rate 0.100 V/s, at different pH; a. 2.8, b. 8.2, c. 3.78, d. 4.56, e. 5.72 and f. 7.4, and the inserted figure shows the relation of the peak potential with the pH of the solution for both cathodic and anodic peaks.

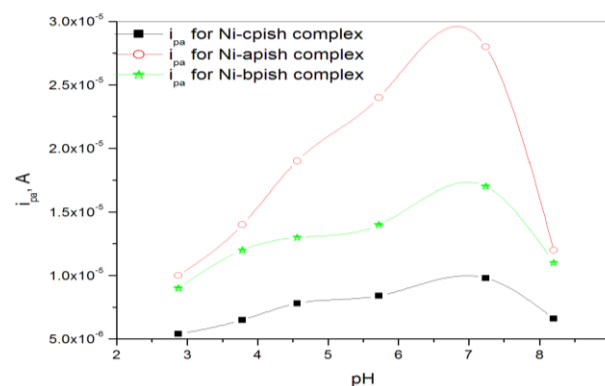


Fig. (5), Relation of pH on the peak current, i_p , for the cyclic voltammetry of Ni-complexes

3.1.3. Effect of Concentration

Fig. (6), represents the effect of changing the concentration of the $[\text{Ni}(\text{cpish})(\text{H}_2\text{O})]\text{Cl}_2 \cdot 2\text{H}_2\text{O}$ complex, as a representative example, on the cyclic voltammetry at pH of 7.4 universal buffer solution. Both of the cathodic and the anodic peaks are observed in the whole concentration range of the study from 2 to 12 μM . The dependence of the voltammetric peak current, i_p , of both anodic and cathodic peaks, i_{pa} and i_{pc} , on the Ni(II) isatin-hydrazone complexes concentration was recorded.

It is found that, the peak current, i_p , increased with increasing the concentration of the complexes, c.f. the

inserted figure in fig. (6). The least squares fit obtained can be formulated as follows;

$$i_{pc} = -6.9 \times 10^{-4} - 0.56 C, \quad r = 0.964 \text{ (cathodic peak)}$$

$$i_{pa} = 0.0012 + 0.53 C, \quad r = 0.980 \text{ (anodic peak)}$$

These equations revealed that, the electrode processes are diffusion controlled, which indicated that, the electrochemical behavior of the subject complexes exhibited no adsorption complications.

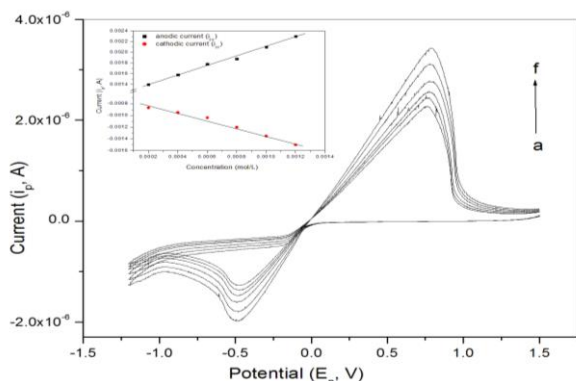


Fig. (6), Cyclic voltammogram of $[\text{Ni}(\text{cpish})(\text{H}_2\text{O})]\text{Cl}_2 \cdot 2\text{H}_2\text{O}$ complex in 10% aqueous methanol (v/v) universal buffer at pH 7.4, at different concentrations; a, 2, b, 4, c, 6, d, 8, e, 10 and f, 12 μM , at scan rate of 0.100 V/s, and the inserted figure showed the relation of the peak current for both cathodic and anodic wave with changing the concentration.

3.1.4. The mechanism of the electron transfer process

Fig. (1), demonstrate the cyclic voltammograms of the $[\text{Ni}(\text{cpish})(\text{H}_2\text{O})]\text{Cl}_2 \cdot 2\text{H}_2\text{O}$ complex, Ni-cpish, as representative example, at glassy carbon electrode at pH 7.4, at different scan rates (0.08 -1.0 V s^{-1}) and in a potential sweep range from 1.5 to -1.4 volt.

It is obvious that, there is one cathodic cyclic voltammetric peak in the forward direction which shifts to more negative value with increasing the scan rate and one anodic cyclic voltammetric peak in the reverse direction which shifts to more positive value with increasing the scan rate. The peak to peak separation (ΔE_p) of these couple is in the range of ≈ 1.0 to 1.3 V, which increased with increasing the scan rates, so, we can considered the two waves are two independently irreversible cyclic voltammetric waves. The number of electrons transferred (n) could be obtained using the following equation:

$$|E_p - E_{p/2}| = \frac{1.857RT}{\alpha nF} = \frac{0.048}{\alpha n} V = \frac{48}{\alpha n} \text{ mV}$$

Where E_{pc} is the peak potential, $E_{p/2}$ is the half peak potential, α is the electron transfer coefficient (generally, $0.3 < \alpha < 0.7$), F is Faraday constant (96487 coulombs/mol), R universal gas constant (8.314 J/K/mol) and T is Kelvin temperature. In the present study, the value of $|E_p - E_{p/2}| \approx 0.09 - 0.10$ V, *c.f.* Table (1), thus the value of n was calculated to be ≈ 1 , on assuming α equals 0.5 for an irreversible process, suggesting that, the Ni(II) complexes exhibits irreversible one electron transfer process.

Table (1), cyclic voltammetric data of cathodic and anodic peaks of the Ni(II) isatin-hydrazone complexes at different scan rates, v , and at 298 K.

| Complex | $v, \text{V/s}$ | Cathodic wave | | | | | | Anodic wave | | | | | |
|------------------|-----------------|----------------------|-------------------|-----------------------|--------------------|-----------------|------------------------------------|----------------------|-------------------|-----------------------|--------------------|-----------------|------------------------------------|
| | | $I_p^c, \mu\text{A}$ | E_p^c, V | $E_{p/2}^c, \text{V}$ | $E_{pc}-E_{p/2}^c$ | $I_p^c/v^{1/2}$ | $D, 10^{-6} \text{ cm}^2/\text{s}$ | $I_p^a, \mu\text{A}$ | E_p^a, V | $E_{p/2}^a, \text{V}$ | $E_{pa}-E_{p/2}^a$ | $I_p^a/v^{1/2}$ | $D, 10^{-6} \text{ cm}^2/\text{s}$ |
| | | | | | | | | | | | | | |
| Ni-cpish complex | 0.08 | 7 | -0.500 | -0.590 | 0.090 | 24.74 | 0.220 | 14 | 0.760 | 0.662 | 0.098 | 49.49 | 0.884 |
| | 0.10 | 8.5 | -0.535 | -0.633 | 0.098 | 26.87 | 0.260 | 15 | 0.811 | 0.721 | 0.090 | 47.43 | 0.812 |
| | 0.20 | 9.8 | -0.620 | -0.717 | 0.097 | 21.91 | 0.173 | 17 | 0.825 | 0.725 | 0.100 | 38.01 | 0.521 |
| | 0.50 | 12 | -0.700 | -0.800 | 0.100 | 16.97 | 0.104 | 19.9 | 0.910 | 0.810 | 0.100 | 28.14 | 0.286 |
| | 0.80 | 14 | -0.754 | -0.859 | 0.105 | 15.65 | 0.088 | 21 | 0.970 | 0.865 | 0.105 | 23.47 | 0.199 |
| | 1.00 | 16 | -0.790 | -0.890 | 0.100 | 16 | 0.092 | 24 | 1.060 | 0.950 | 0.110 | 24 | 0.208 |
| Ni-apish complex | 0.08 | 33 | -0.522 | -0.620 | 0.098 | 116.67 | 4.911 | 36 | 0.712 | 0.622 | 0.090 | 127.27 | 5.845 |
| | 0.10 | 35 | -0.550 | -0.640 | 0.090 | 110.67 | 4.420 | 38 | 0.730 | 0.625 | 0.105 | 120.16 | 5.210 |
| | 0.20 | 40 | -0.650 | -0.750 | 0.100 | 89.44 | 2.886 | 42 | 0.765 | 0.665 | 0.100 | 93.91 | 3.182 |
| | 0.50 | 48 | -0.780 | -0.885 | 0.105 | 67.88 | 1.663 | 50 | 0.950 | 0.850 | 0.100 | 70.71 | 1.804 |
| | 0.80 | 51 | -0.855 | -0.955 | 0.100 | 57.019 | 1.173 | 55 | 1.100 | 0.990 | 0.110 | 61.49 | 1.364 |
| | 1.00 | 54 | -0.930 | -1.040 | 0.110 | 54 | 1.052 | 58 | 1.160 | 1.050 | 0.110 | 58 | 1.214 |
| Ni-bpish complex | 0.08 | 13 | -0.450 | -0.547 | 0.097 | 45.96 | 0.762 | 21 | 0.680 | 0.590 | 0.090 | 74.24 | 1.989 |
| | 0.10 | 15 | -0.480 | -0.580 | 0.100 | 47.43 | 0.812 | 24 | 0.750 | 0.660 | 0.090 | 75.89 | 2.078 |
| | 0.20 | 17 | -0.514 | -0.619 | 0.105 | 38.01 | 0.521 | 26 | 0.790 | 0.692 | 0.098 | 58.13 | 1.220 |
| | 0.50 | 20 | -0.590 | -0.695 | 0.105 | 28.28 | 0.289 | 29 | 0.820 | 0.720 | 0.100 | 41.01 | 0.607 |
| | 0.80 | 23 | -0.640 | -0.750 | 0.110 | 25.71 | 0.239 | 32 | 0.920 | 0.820 | 0.100 | 35.77 | 0.462 |
| | 1.00 | 26 | -0.690 | -0.800 | 0.110 | 26 | 0.244 | 37 | 1.030 | 0.920 | 0.110 | 37 | 0.494 |

3.2. The interaction of the Ni(II)-complexes with CT-DNA using cyclic voltammetry.

3.2.1. The effect of addition of CT-DNA with the Ni(II) complexes

The application of the cyclic voltammetric technique to the study of interaction between the metal complexes and DNA provides a useful complement to the previously used spectral and viscometric studies [26]. The use of cyclic voltammetry to the study of the metal complex-DNA interaction is due to it's simply, faster and needed less samples. In the present work, cyclic voltammetry has been used to study the interaction of the subject redox active Ni(II) complexes with DNA with a view to further explore the DNA-binding models assessed from the previously spectral and viscometric methods. Typical CV curves for 0.1 mM [Ni(cpish)(H₂O)]Cl₂·2H₂O complex, as representative example, in 10% (v/v) aqueous-methanol (universal buffer) at Glassy carbon electrode, in the absence and in the presence of CT-DNA are shown in *fig. (7)*. In the absence of CT-DNA, the cathodic peak potential, E_{pc} , appeared at -0.535 V and the anodic one, E_{pa} , at 0.84 V. No new redox peaks appeared after the addition of CT-DNA to the subject complex, but results in; (1) a shift of the cathodic and anodic peak potentials to more positive values and (2) a decrease of the cathodic and anodic peak currents.

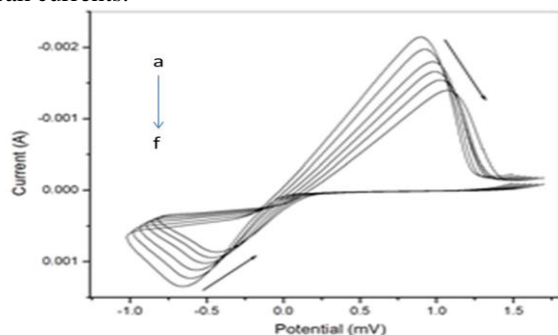


Fig. (7), Cyclic voltammogram of [Ni(cpish)(H₂O)]Cl₂·2H₂O complex in 10% aqueous methanol (v/v) universal buffer at pH 7.4 and scan rate 0.100 V/s at different concentrations of CT-DNA; a. 0, b. 10, c. 20, d. 30, e. 40 and f. 50 μ M.

Typical voltammetric data of the cathodic and anodic peak potentials and the shift of the potentials in the absence and presence of CT-DNA of the subject complex at different CT-DNA concentrations, given in terms of the relative concentration, R , and the concentration of CT-DNA, [DNA], where $R = [\text{DNA}]/[\text{Ni(II) complex}]$, are summarized in *table (2)*.

In the presence of 10 μ M CT-DNA, $E_{pc} = -0.411$ V and $E_{pa} = 0.945$ V. Thus the E_{pc} shows a positive shift ($\Delta E_{pc} = +124$ mV) and E_{pa} shows a positive shift ($\Delta E_{pa} = +134$ mV). These shifts in the peak potentials confirm that the subject complexes can bind to CT-DNA by intercalation binding mode [27]. The effect of, R , on both the E_{pc} and E_{pa} values are shown in *fig. (8)*.

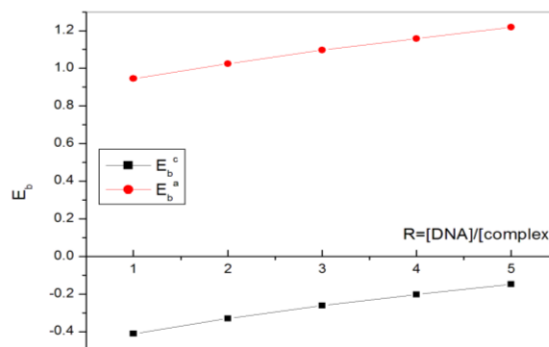


Fig. (8), the effect of, R , on both the E_{pc} and E_{pa} values

Furthermore, in the presence of an excess of CT-DNA, the current intensity of all the peaks (i_{pc} and i_{pa}) decreased significantly, suggesting the existence of an interaction between the subject complexes and the CT-DNA. The decrease in the current intensity can be explained in terms of an equilibrium mixture of free and CT-DNA-bound complex to the electrode surface [28]. This decrease is due to that the diffusion coefficient of the subject complex when bound to the CT-DNA is some smaller than that of the free complex. The free and bound diffusion coefficients, D_f and D_b , for [Ni-cpish complex] were determined by CV, *c.f. fig. (8)*.

Table (2), the cathodic and anodic peak potentials and the shift of the potentials in the absence and presence of CT-DNA.

| | [DNA], μ M | | | | | | | | | | | [DNA], μ M | | | | | | | | | | | | |
|-----------|-----------------------------|-----------------------------|--|-----------------------------|--|-----------------------------|--|-----------------------------|--|-----------------------------|--|-----------------------------|-----------------------------|--|-----------------------------|--|-----------------------------|--|-----------------------------|--|-----------------------------|--|----|--|
| | 0 | | 10 | | 20 | | 30 | | 40 | | 50 | | 0 | | 10 | | 20 | | 30 | | 40 | | 50 | |
| | E _f ^c | E _b ^c | Δ E _{b-0} ^c | E _b ^c | Δ E _{b-0} ^c | E _b ^c | Δ E _{b-0} ^c | E _b ^c | Δ E _{b-0} ^c | E _b ^c | Δ E _{b-0} ^c | E _f ^c | E _b ^a | Δ E _{b-0} ^a | E _b ^a | Δ E _{b-f} ^c | E _b ^a | Δ E _{b-f} ^c | E _b ^a | Δ E _{b-f} ^c | E _b ^a | Δ E _{b-f} ^c | | |
| Ni-cpi sh | -0.535 | -0.411 | 0.124 | -0.303 | 0.205 | 0.2061 | 0.2074 | -0.202 | 0.3033 | -0.1048 | 0.3087 | 0.811 | 0.945 | 0.134 | 1.024 | 0.213 | 1.097 | 0.286 | 1.158 | 0.347 | 1.219 | 0.408 | | |
| Ni-api sh | -0.505 | -0.426 | 0.124 | -0.346 | 0.204 | 0.2074 | 0.2076 | -0.202 | 0.3037 | -0.1057 | 0.3093 | 0.703 | 0.877 | 0.147 | 0.957 | 0.227 | 1.027 | 0.297 | 1.086 | 0.356 | 1.148 | 0.418 | | |
| Ni-bpi sh | -0.408 | -0.365 | 0.115 | -0.284 | 0.196 | 0.2012 | 0.2068 | -0.1055 | 0.3025 | -0.0098 | 0.3082 | 0.705 | 0.874 | 0.124 | 0.955 | 0.205 | 1.025 | 0.275 | 1.085 | 0.335 | 1.146 | 0.396 | | |

3.2.2. To find out the complex-DNA binding constant.

The gradual decay in both cathodic and anodic peak currents, i_{pc} and i_{pa} , of the complexes by the addition of varying concentration of DNA, ranging from 10 to 50 μM , can be used to quantify the binding constant by using the following equation [29]:

$$\log\left(\frac{1}{[DNA]}\right) = \log k + \log\left(\frac{I_{\text{complex-DNA}}}{I_{\text{free complex}} - I_{\text{complex-DNA adduct}}}\right)$$

Where, K is the binding constant, I_G and I_{H-G} are the peak currents of the free complex (G) and the complex-DNA adduct (H-G), respectively. The binding constant for the interaction of Ni(II) isatin-hydrazone complexes with CT-DNA were obtained from the intercept of $\log(1/[DNA])$ versus

$$\log\left(\frac{I_{\text{complex-DNA}}}{I_{\text{free complex}} - I_{\text{complex-DNA adduct}}}\right) \text{ plots, c.f. table (3).}$$

Table (3), the intrinsic binding constants, k_b , Gibbs free energy, ΔG and Diffusion coefficient, D , for the interaction between DNA and Ni(II) complexes.

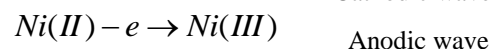
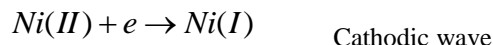
| | Binding constant “ K_b , M^{-1} ” | | Gibbs free energy ΔG (kJmol^{-1}) | | Diffusion coefficient D , $10^{-6}\text{cm}^2/\text{s}$ | | | |
|----------|--|-----------------------|---|------------------|--|-------|---------------|-------|
| | From i_{pc} | From i_{pa} | From i_{pc} | From i_{pa} | From i_{pc} | | From i_{pa} | |
| | | | | | D_f | D_b | D_f | D_b |
| Ni-cpish | 1.22 $\times 10^4$ | 1.45 $\times 10^4$ | - 23.31 | - 23.74 | 4.42 | 3.58 | 5.21 | 4.21 |
| Ni-apish | 6.75 $\times 10^3$ | 6.54 $\times 10^3$ | - 21.84 | - 21.76 | 0.812 | 0.53 | 2.078 | 1.35 |
| Ni-bpish | 2.12 $\times 10^4$ | 1.89 $\times 10^4$ | - 24.68 | - 24.39 | 0.26 | 0.12 | 0.812 | 0.54 |

The values of binding constants values calculated from the decay in both cathodic and anodic peak currents, i_{pc} and i_{pa} , indicate that these complexes bind with CT-DNA in both forward and backward directing of the CV voltaammgram with the same extent. The negative values of standard Gibbs free energy ($\Delta G = -RT \ln K_b$) indicate the spontaneity of the binding interaction of these complexes with DNA.

4. Conclusion

The electrochemical behavior of the Ni(II) isatin-hydrazone complexes have been investigated in 10% aqouse-methanol, v/v, of Britton–Robinson buffer “universal buffer” as supporting electrolyte at Glassy carbon electrode. It is obvious that, there is one cathodic cyclic voltammetric peak in the forward direction which shifts to more negative value with increasing the scan rate and one anodic cyclic voltammetric peak in the reverse direction which shifts to more positive value with increasing the scan rate. The peak to peak separation (ΔE_p) of these couple is in the range of ≈ 1.0 V, which increased with increasing the scan rates, so, we

can considered the two waves are two independently irreversible cyclic voltammetric waves. The cathodic wave represents an irreversible reduction of Ni(II) to Ni(I) by an irreversible electron transfer process, in the anodic process, the Ni(II) undergoes an irreversible oxidation to Ni(III) by an irreversible electron transfer process.



One strategy for the development of drugs and chemotherapeutic agents involves medicinal candidates which interact reversibly with DNA through non-covalent interactions. The binding of the Ni(II) isatin-hydrazone complexes to DNA has been characterized through cycling voltammetric analysis. From the correlation of the used technique, the interaction mode between the Ni(II) isatin-hydrazone complexes and CT-DNA can be elucidate to be intercalation binding. Moreover, the binding constant which measure of compound–DNA complex stability was evaluated for these compounds, The overall binding constant values are comparable to that of typical intercalators such as isoxazocucu-mine ($6.3 \times 10^3 M^{-1}$) and lumazine ($1.74 \times 10^4 M^{-1}$) and revealed stronger interaction of investigated compounds with DNA via intercalation mode.

References

- [1] W. Kaim, B. Schwederski. Bioinorganic Chemistry: Inorganic Elements of Life, John Wiley and Sons: London. 1996:39-262pp.
- [2] C. Xiao-Ming, Y. Bao-Hui, C.H. Xiao, X.J. Zhi-Tao. Chem. Soc., Dalton Trans.1996:3465-3468.
- [3] F.A. Cotton, G. Wilkinson. Advanced Inorganic Chemistry, 5th ed., John Wiley and Sons: New York. 1988:1358-1371pp.
- [4] N.N. Greenwood, A. Earnshaw. Chemistry of the Elements, Pergamon Press: Oxford. 1984:1392-1420pp.
- [5] Sarangapani, M.; Reddy, N. A.; Jayamma, Y.; Reddy, V. M.Indian Drugs 1998, 35, 336.
- [6] Bhattacharya, S. K. Indian J. Exp. Biol. 1998, 36, 118.
- [7] Singh, G. S.; Singh, T.; Lakhan, R. Indian J. Chem., Sect. B 1997, 36, 951.
- [8] Lingaiah, N.; Narendra, R.; Dattatray, A. M. Indian J. Chem., Sect. B 1998, 37, 1254.
- [9] Medvedec, A. E.; Clow, A.; Sandler, M.; Glover, V. Biochem. Pharmacol 1998, 52, 385.
- [10] Panova, N. G.; Zemskova, M. A.; Axenova, L. N.; Medvedev, A. E. Neurosci. Lett. 1997, 223, 58.
- [11] Silva, J. F., Garden, S. J., Pinto, A. C., J. Braz. Chem. Soc. 2000,12, 3.
- [12] Pandeya, S. N.; Smitha, S.; Stables, J. P. Arch. Pharm. Med. Chem. 2002, 4, 129-134.
- [13] Pandeya, S. N.; Sriram, D.; Yogeeswari, P.; Ananthan, S. Chemotherapy 2001, 47, 266-269.

- [14] Brewerton, T. D.; Zealberg, J. J.; Lydiard, R. B.; Glover, V.; Sandler, M.; Ballenger, J. C. *Biol. Psychiatry* 1995, 37, 481-483.
- [15] S.C. Nayak, P.K. Doss and K. Sahoo. *J.Anal.Appl.Pyrolysis*. 2003; 70:699-709.
- [16] Rabia, M. K.; M. M. ohamad, A. D.; I. smail, N. M.; Mahmoud, A. A. *Russ J Gen Chem* 2013, 83(12): 2406–2412.
- [17] Rabia, M. K.; M. M. ohamad, A. D.; I. smail, N. M.; Mahmoud, A. A. *Russ J Gen Chem* 2013, 83(12): 2502–2509.
- [18] Rabia, M. K.; M. M. ohamad, A. D.; I. smail, N. M.; Mahmoud, A. A. *J Iran Chem Soc* 2014, 11(4): 1147–1163
- [19] Bard, A. J. and Faulkner, L. R., *Electrochemical Methods, Fundamentals and Applications*, John Wiley and Sons, New York, [2001].
- [20] Hrapovic, S., and Luong, J. H. T. *Anal. Chem.*, 75, 3308 [2003].
- [21] de Souza, J. R.; de Castro, C. S. P.; Jr, C. B., *J. Braz. Chem. Soc.* 2000, 11, 314
- [22] Guin, P. S.; Das, S., *International Journal of Electrochemistry*, 2014, 2014, 1-8.
- [23] R. S. Nicholson, *Anal. Chem.* 37, 1351 (1965)
- [24] A.J. Bard and L.R. Faulkner (Eds), *Electrochemical Methods: Fundamentals and Applications*, 2nd edit., Wiley, New York, (2001).
- [25] Mahadevan, S., Palaniandavar, M., *Inorg. Chem.* 37 (1998) 693–700
- [26] Michael, Rodriguez M., Bard A. J., *J. An. Chem. Soc.*, 111 (1989) 8901-8911.
- [27] Tabssum S., Parveen S., Arimand F., *Acta Biomater.*, 1 (2005) 677-689.
- [28] L.-S. Feng, M.-L. Liu, B. Wang, Y. Chai, X.-Q. Hao, S. Meng, H.-Y. Guo, *Eur. J. Med. Chem.* 45 (2010) 3407–3412.